ACS OMEGA

http://pubs.acs.org/journal/acsodf

Review

Review of Molybdenum Disulfide Research in Slurry Bed Heavy Oil Hydrogenation

Xiaoning Zhang, Buning Chen, Jianwei Wang, Yusheng Zhou, Xueli Huang,* He Huang, Xuefeng Wang, and Kaihong Li

Cite This: *ACS Omega* 2023, 8, 18400−18407

Read Online

ABSTRACT: With the growing demand for gasoline and diesel fuel and the shortage of conventional oil reserves, there has been extensive interest in upgrading technologies for unconventional feedstocks such as heavy oil. Slurry bed reactors with high tolerance to heavy oil have been extensively investigated. Among them, dispersive MoS_2 is favored for its excellent hydrogenation ability for heavy oil even under harsh reaction conditions such as high pressure and high temperature, its ability to effectively prevent damage to equipment from deposited coke, and its ability to meet the requirement of high catalyst dispersion for slurry bed reactors. This paper reviews the relationship between the structure and hydrogenation effectiveness of dispersive molybdenum disulfide, the hydrogenation mechanism, and the improvement of its hydrogenation performance by adding defects and compares the application of molybdenum disulfide in heavy oil hydrogenation, desulfurization, deoxygenation, and denitrification. It is found that the current research on dispersive molybdenum disulfide catalysts focuses mostly on the reduction of stacking layers and catalytic performance, and there is a lack of research on the lateral dimensions, microdomain regions, and defect sites of MoS_2 catalysts. The relationship between catalyst structure and hydrogenation effect also lags far behind the application of MoS_2 in the precipitation of hydrogen, etc. Oil-soluble and water-soluble MoS_2 catalysts eventually need to be converted to a solid sulfide state to have hydrogenation activity. The conversion history of soluble catalysts to solid-type catalysts and the key to their improved catalytic effectiveness remain unclear.

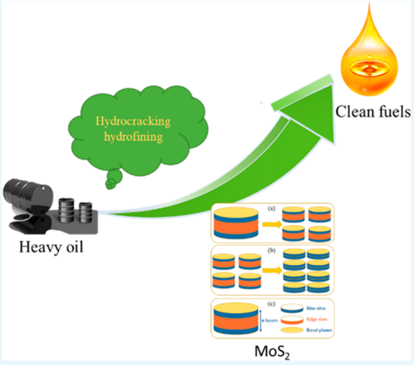

1. INTRODUCTION

In recent years, the growing demand for greener and lighter fuels, the shortage of crude oil reserves, and the shrinking conventional oil have created an urgent need to develop heavy oil refining technologies to ensure national defense security and national interests. In the field of petroleum catalyst hydrogenation, most of the research has focused on the advancement of refining technologies for low-quality industrial products (e.g., depressurized residual oil, coal tar, etc.) as well as unconventional oils (e.g., superheavy oil, oil sands, etc.), which are considered as alternative energy sources.[1] With the rapid growth of global oil consumption, heavy or superheavy oil refineries will be substituted for refineries.[2,3]

Heavy oils usually contain high concentrations of heteroatoms (S, N, and O), transition metals (V, Ni, Fe, and Si), and complex molecules that are responsible for catalyst deactivation and coking in heavy oil refining.[4] Depending on the polarity, heavy oils can be classified as saturates, aromatics, resins, and asphaltenes. The ultimate goals of hydroconversion of heavy crude oils are to reduce viscosity, remove heteroatoms, inhibit coking, increase the H/C ratio required for commercial products, and reduce hazards such as air pollution and acid rain during fuel consumption.

Catalytic hydroconversion is a more efficient way to upgrade heavy oil into liquid transportation fuels for modern refineries. Various hydrogenation reactor technologies using a fixed-bed, boiling-bed, moving-bed, and slurry-bed have been designed for the hydroconversion of heavy oils. Hydroprocessing using fixed-, boiling-, or moving-bed reactors often has the disadvantage of coking and heavy metal deposition leading to catalyst deactivation, especially for the hydroprocessing of heavier feedstocks. In addition, there are critical issues such as feed diffusion, pressure drop, and mass transfer in fixed-, boiling-, or moving-bed reactors. Slurry-bed reactors can overcome the limitations of these processes.[5,6] Effective catalysts for the conversion of heavy oils into high-value products with lower boiling points by hydroconversion processes have been extensively studied for more than 50 years. Among these catalysts, MoS_2 is favored as one of the

Received: March 28, 2023
Accepted: May 4, 2023
Published: May 15, 2023

https://doi.org/10.1021/acsomega.3c02029
ACS Omega 2023, 8, 18400−18407

main active catalysts due to its superior hydrogenation ability for heavy oils (including high sulfur content, impurities, and heavy components) even under harsh reaction conditions such as high pressure and high temperature and its ability to effectively stop the damage caused by deposited coke to the equipment. Although alumina-loaded Ni−Mo and Co−Mo nonhomogeneous catalysts have been used in fixed-bed and fluidized-bed reactors, unsupported Mo-based dispersion catalysts are used in slurry-bed reactors because of their strong resistance to deactivation, coking inhibition, and no diffusion limitation of reactants

2. MOS_2 CATALYST

MoS_2 has numerous physicochemical properties and has several potential applications such as tribology, hydrogen precipitation reactions (HERs),[7−11] lithium-ion batteries, and microelectronics[12,13] and as a major catalyst in heavy oil refining processes.[14] MoS_2 crystals belong to the hexagonal crystal system and have three different forms of configuration such as 1T (a = 5.60 Å and c = 5.99 Å), 2H (a = 3.15 Å and c = 12.30 Å), and 3R (a = 3.17 Å and c = 18.38 Å).[15,16] The 3R phase exhibited better catalytic activity than the 2H and 1T phases in hydrogen precipitation reactions,[17] and the 2H phase was mainly applied in heavy oil hydrogenation. The thermodynamically stable and naturally occurring MoS_2 is 2H (3% 3R content).[18] Two of the substable states, 1T-MoS_2 and 3R-MoS_2, can be converted to the stable 2H-MoS_2 form at high temperatures. In the UV−vis spectrum, 2H-MoS_2 shows two significant peaks at ($\lambda \sim 580$ nm) 2.1 eV and ($\lambda \sim 640$ nm) 1.9 eV.[19]

The MoS_2-catalyzed hydrogenation model, the Rim-edge model, was first proposed by Daage. The Rim-edge (Figure 1) model states that the basal atom is not reactive; the Rim atom is the active center of the hydrogenation reaction and the hydrodesulfurization reaction; and the Edge atom is the active center of the hydrogenation reaction. As shown in Figure 1a, when MoS_2 catalysts have the same longitudinal dimensions, MoS_2 with smaller lateral dimensions can expose more edges and exhibit higher catalytic hydrogenation activity. Figure 1b shows that MoS_2 catalysts with the same lateral dimensions and different numbers of stacked layers show the same number of exposed edges, but MoS_2 catalysts with fewer stacked layers show more catalytic activity (similar to mechanical stripping). That is, not all exposed edges of the S−Mo−S atomic layer are used as active sites for catalytic hydrogenation, while only the Rim atom is used as catalytically active sites for PAH hydrogenation. Therefore, it can be speculated that only the Rim atom has stronger catalytic hydrogenation activity. The MoS_2 catalysts with theoretical minimum lateral size and stacked layers of 2 have the highest hydrogenation activity.[5,20]

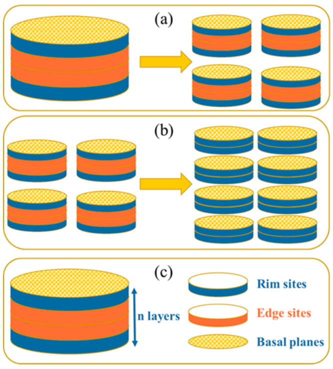

Figure 1. MoS_2 model: (a) the same stacked layers and different lateral dimensions, (b) the same lateral dimensions and different stacked layers, and (c) Rim-edge model.

Hydrogen molecules can be adsorbed at the edge positions of MoS_2 and dissociate into hydrogen atoms bound to S^{2-} or Mo atoms, forming acidic SH groups and metal hydrides.[21−23] Metal hydride species (e.g., Mo−H) are not thermodynamically favored. Therefore, after the initial H_2 dissociation, hydride species can react with adjacent S^{2-} to form additional SH groups.[24,25] Molecular hydrogen dissociation and atomic hydrogen surface migration can occur in the edge planes of MoS_2 catalysts.[26,27]

The catalytic hydrogenation activity of MoS_2 catalysts is not directly related to the physical properties of the BET surface area. The BET surface area does not determine the catalytic hydrogenation activity of MoS_2 catalysts.[28] However, the MoS_2 substrate surface has good lubricity and photocatalytic activity.[29]

According to DFT calculations and STM studies, planar molecules with π-bond−polycyclic aromatic hydrocarbons can be adsorbed in parallel on the basal plane of MoS_2 through strong van der Waals interactions.[30,31] Hydrogenation may occur in the region located at the edge of the basal plane, where the SH group provides hydrogen. Only the activated H species at the Rim site can react with the polycyclic aromatic hydrocarbons adsorbed on the basal plane.[32] Due to the spatial site resistance effect, the activated H species at the Edge position is difficult to react with PAHs. Accordingly, the Rim site can activate H_2 and, at the same time, facilitate the reaction between activated H species and PAH molecules due to its accessibility. As the hydrogenation of PAHs proceeds, the deep hydrogenation products are nonplanar. Compared to Edge sites, macromolecules have a much smaller spatial site-blocking effect on Rim sites.[33,34] In addition, PAHs can be adsorbed on the whole substrate; however, it is possible that only PAH molecules on the edge of the substrate near the edge sites can hydrogenate with SH at the edge sites, and the aromatic molecules adsorbed at positions far from the edge cannot react with SH. Therefore, the Rim position favors the adsorption of PAHs and the desorption of the corresponding products during catalytic hydrogenation.[5] In addition, Iwata et al. found that the addition of Ni, for example, enhanced the number of inflection points in the substrate and greatly enhanced the MoS_2 catalytic hydrogenation activity.[35]

3. MOS_2 DEFECTS

Typically, 0D point defects of MoS_2 mainly include vacancies and heteroatom replacement defects. The presence of vacancies distorts the lattice and thus effectively modulates the electrical structure and chemical properties of the material. The formation energies of several vacancies, including Mo vacancies (VMo), S vacancies (VS), and mixed Mo and S vacancies ($VMoS_3$), were calculated based on density functional theory by Barik et al. The results show that VS has the lowest formation energy, which is consistent with the frequently observed experimental results. Heteroatom doping by introducing substituted atoms is a common strategy for altering the microscopic morphology, structure, and electrical properties of MoS_2 materials. Heteroatoms include both metallic and nonmetallic elements.[36]

Table 1. Summary of Literature on Heavy Oil Hydrogenation

Type	Oil	Catalytic conditions	Catalysts	Effects	Source
Solids	Iranian heavy oil	200 °C, 6.0 MPa, 24 h	SiO_2-C/MoS_2	81% reduction in viscosity and a 7.7° increase in API	37
Solids	Light-circulating oil	375 °C, 10.3 MPa	Dispersed MoS_2	-	38
Solids	Pineapple oil and palm oil	330 °C, 5.0 MPa, 1.5 h^{-1}	NiMo/γ-Al_2O_3,	Deoxygenation rate: 94.6	39
Solids	Dibenzothiophene	320 °C, 3.0 MPa, 1 h	$MoS_2/SiO_2/Fe_3O_4$	Conversion rate: 80%	40
Water-soluble	Light cycle oil + bio-oil	360 °C, 7.9 MPa, 0.72 h^{-1}	Ammonium secamolybdate tetrahydrate	Oxygen removal rate: 90%	41
Solids	Straight-run gasoline	350 °C, 5.5 MPa, 750 rpm, 3 h	Dispersed MoS_2	HDS: 56%. Commercial CoMo/Al_2O_3: 52−53%	42
Solids	Nitrobenzene	3.0 MPa, 100 °C, 6 h	Dispersed MoS_2	100% conversion (commercial catalyst 52%)	43
Solids	Anthracene/phenanthrene	350 °C, 6−8.0 MPa, 4 h	Dispersed MoS_2	Conversion rate: 56.8, 68.9	5
Solids	Thiophene/pyridine	300 °C, 1 h	MoCoS/MoNiS	Conversion rate: 80% and 50%	44

The extended layer spacing of layered MoS_2 nanosheets is defined as two-dimensional planar defect engineering. The reduction of stacked layers can greatly enhance their hydrogenation properties and improve structural stability during cycling. Typically, the introduction of small molecules, ions, particles, etc. can significantly improve the interlayer distance. About 60% of the interlayer expansion is caused by the introduction of oxygen from Mo precursors or by the insertion of NH^{4+} ions released by thiourea decomposition compared to pristine 2H-MoS_2.[36]

4. MOS$_2$ IN HEAVY OIL HYDROGENATION

Heavy oils are mainly composed of irregularly structured macromolecular compounds with structures including, for example, paraffin, naphthenes, and aromatic hydrocarbons with different physicochemical properties (Table 1). Asphaltenes are the heaviest aromatic component of heavy oils but are the least reactive in destructive hydrogenation reactions, with a percentage of 8−15%. The rapid hydrogenation of asphaltenes is a key step in the conversion of heavy oils into clean fuels.[28] According to the Yen Mullins model,[45,46] asphaltene molecules form asphaltene nanoaggregates through intermolecular forces with aggregates of 6. These nanoaggregates can further aggregate to form aggregates of 8. The asphaltene molecular structure is usually considered a “continental” or “archipelagic” model.[28]

Asphaltenes cause the following problems during the thermal treatment of heavy oils: (1) Asphaltenes not only adversely affect the overall rate of the HDT reaction but also limit the maximum degradation during the thermal treatment of heavy oils. (2) During catalytic hydrogenation, asphaltene stability decreases, which in turn leads to a shift to coke resulting in catalyst deactivation and, in severe cases, clogging of the reactor.[47]

Heavy oil macromolecules are easily activated at a higher reaction temperature, which is conducive to asphaltene hydrocracking and asphaltene composition changes with the increase in reaction temperature. In this process, the side chains of asphaltene molecules are easily removed, and the remaining thickened aromatic rings form larger molecules through dehydrogenation and condensation, thus generating coke.[4] It is easy to activate at higher reaction temperatures, which is conducive to hydrolysis and cracking reactions. When the reaction temperature reached 410 °C, nearly 60% of the asphaltene in the feedstock was converted. This not only indicates that high reaction temperature is beneficial to asphaltene hydrocracking but also indicates that asphaltene composition changes with the increase in reaction temperature. At high temperatures, part of the alkyl side chains of asphaltene macromolecules are removed, and the remaining thickened aromatic rings react with each other through dehydrogenation and condensation to form larger molecules, thus increasing coke and gas generation.[4] Meanwhile, the conversion of sulfur and oxygen follows an almost linear trend as the reaction temperature increases. The sulfur content decreases due to the destruction of the sulfur bridges on the alkyl chains. However, the nitrogen content in asphaltenes first decreases and then does not change significantly. Nitrogen compounds in asphaltene structure are one of the most difficult heteroatoms to deal with. The HDT of these compounds is not favorable to thermodynamics and therefore has high stability.[4] Due to the small decomposition energy of the C−S bond, HDS is easier than HDN,[2,48] and the decomposition energy of the C−S bond is smaller than that of other bonds in crude oil molecules. Therefore, these are the first bonds to break down, resulting in a decrease in crude oil viscosity and an increase in API gravity.[37] XRD, ^1H NMR, and XPS analysis of asphaltene showed that with the increase of temperature the molecular weight of asphaltene decreased; the aromaticity increased; and the space between the layers and chains of asphaltene decreased (asphaltene structure became denser). With the increase in reaction temperature, the content of S and molecular weight of asphaltene decreased first, while the content of N decreased first and then changed a little.[4] A comparison of different crude oil samples revealed a relatively uniform distribution of different sulfur molecular groups in heavy oils, and compared to monocyclic and bicyclic aromatics, tricyclic aromatics have a higher tendency to adsorb in hydrotreating catalysts and therefore will strongly compete with sulfur compounds for catalyst sites.[49] Partial hydrogenation of polycyclic aromatic hydrocarbons in heavy oil hydrogenation produces aromatic compounds attached to saturated rings, which are converted sequentially to monocyclic aromatic hydrocarbons by cracking. In the case of residual oil conversion, hydrocracking helps to obtain low boiling point distillates as well as hydrodesulfurization and hydrodenitrogenation.[48]

There are two main forms of MoS_2 catalyst in the slurry bed: solid powder catalyst and dispersion catalyst. The dispersion of solid powder catalysts in crude oil is poor, and it is difficult to provide efficient catalytic hydrogenation. This is overcome by dispersion catalysts. However, from an economic point of view,

https://doi.org/10.1021/acsomega.3c02029

oil-soluble precursors in dispersed catalysts, including molybdenum naphthenate and molybdenum diethyl caproate (molybdenum caprylate), are suitable for the recovery process rather than the primary method. The main function of the catalyst required by the slurry process is not hydrodesulfurization (HDS) but hydrogenation (HYD). At present, the performance of oil-soluble catalysts is close to the maximum. Under the same conditions, hydrogenation of heavy oil without a catalyst can increase the content of asphaltene by 15−20%.[35]

In the hydrogenation of heavy oil, the hydrogenation of polycyclic aromatic hydrocarbons (PAHs) is carried out in successive steps. The first ring hydrogenation kinetics of PAHs is favorable. This result indicates that the hydrogenation rate of the subsequent rings is slower, and the last ring hydrogenation is more difficult compared to the first ring hydrogenation. In the case of anthracene, for example, AN can be hydrogenated first to the preliminary AH2, and the reaction is kinetically very easy even without a catalyst. However, deep hydrogenation will become increasingly difficult. The MoS_2 catalyst with the smallest lateral size and the smallest stacking layer exhibited the highest catalytic activity for the hydrogenation of phenanthrene and naphthalene. According to the GC-MS results, the hydrogenation of polycyclic aromatic hydrocarbons (PAHs) proceeds sequentially: PAHs are first hydrogenated to preliminary products and then further hydrogenated to full saturation. Only trace amounts of hydrocracking products could be detected.[5] The hydrogenation reaction occurs mainly for bicyclic aromatic hydrocarbons, which are reduced to monocyclic compounds; monocyclic and polycyclic aromatic hydrocarbons are almost not hydrogenated. This phenomenon confirms the weak hydrogenation ability of the carrier-free catalysts.[38] Kadiev et al. found through DFT calculation that the catalytic hydrogenation conversion catalyst containing molybdenum and nickel was conducive to reducing the content of asphaltene and resin in the reconversion products. In contrast to the case of molybdenum, benzene molecules are chemically adsorbed to nickel by double bonds.[47] The addition of nickel atoms can improve the stability of the hydrogenated intermediate and promote the hydrogenation of heavy oil.[50]

The mechanism of residue slurry bed hydrocracking is similar to viscosity-reducing cracking in the presence of free radical H_2, and the main reactions in these processes are free radical reactions, including cracking and condensation. Although the addition of molybdenum catalysts is effective in suppressing coking,[51] increasing the catalyst dosage does not always improve the catalytic effect. Li et al. derived the highest Mo^{4+} concentration and colloidal stability of the system after sulfidation for Mo-based catalyst concentrations up to 300 ppm, resulting in the lowest coke yield and highest catalytic hydrogenation performance in the reduced viscous residue passion.[52]

Persi et al. obtained water-soluble Ni−Mo catalysts by preparing mixed solutions at room temperature, resulting in the reduction of crude oil S content from 5.5 to 3.1% and N content from 750 to 392 ppm. The increase of aromatic and saturated hydrocarbon compounds at the expense of asphaltenes and resins increased the volume of gasoline and diesel to 8 and 14%, respectively.[48] Liu et al. dissolved the catalyst precursor cetyltrimethylammonium heptamolybdate The resin fraction decreased from 25.21 wt % to 3.54 wt %, and the C7-asphalt content decreased from 6.82 wt % to almost zero. The yield of liquid products increased from 75.03 wt % to 96.43 wt %.[53] Abdullahi et al. performed catalytic cracking of Oman thick oil with an oil-soluble NiMo viscosity reduction catalyst and glycerol as a hydrogen donor, and the maximum viscosity was reduced by 69% in a 30 h reaction at 277 °C.[54] Since carrier-free MoS_2 is a hydrocracking catalyst without cracking capacity, heavy oil decomposes by thermal cracking during hydroconversion using a dispersion catalyst.[14]

5. MOS_2 IN HEAVY OIL DECONTAMINATION

Due to the burning of light fuels, sulfur dioxide (SO_2) and nitrogen oxides (NOx) are prone to environmental problems such as acid rain. Due to the requirement for environmental protection, most countries have increasingly strict control over the heteroatom content in fuel oil.[55,56]

Carrier-free Mo catalysts were evaluated for hydrodeoxygenation using model compounds such as phenol, methyl phenol, and methoxyphenyl.[57,58] These carrier-free Mo catalysts were found to favor the direct deoxygenation pathway.[59] Hydrotreating of hydrothermal liquefied bio-oil using carrier-free catalysts showed hydroxyl removal rates comparable to those of commercial NiMo/γ-Al_2O_3. Hydrodeoxygenation leads to a decrease in oxygen content and a decrease in acidity. After hydrotreating, the atomic O/C ratio decreased significantly, while the effective H/C of the feed mixture increased slightly from 1.07 to 1.26 to 1.23−1.31. The significant decrease in O/C can be attributed to hydrodeoxygenation, and the slight increase in the H/C ratio implies limited ring saturation of the oil product.[41] Carrier-free MoS_2 catalysts with low stacking are more selective for the hydrogenation of C−OH bonds in phenol molecules, while MoS_2 with high stacking is more favorable for the hydrogenation of aromatic rings.[59] Co-MoS_2 with nanoflower morphology exhibited higher *p*-cresol conversion performance (rate constant of 0.37 h^{-1}) compared to Co-MoS_2 with nanotube morphology (rate constant of 0.23 h^{-1}). The reason for the improved catalytic performance of Co-MoS_2 with nanoflower morphology can be attributed to the presence of various exposed edges and the synergistic effect between Co- and MoS_2-based nanomaterials.[60,61] These studies were analyzed using the atom-vacancy interface model and found that isolated cobalt atoms promote hydrogen activation and that the underlying sulfur atoms promote carbon−oxygen fracture and vacancy regeneration.[62] Zhang et al. hydro-deoxidized fatty acids and triglycerides to produce diesel fuel. Based on the equilibrium constant of the reverse water-vapor transfer reaction, it is indicated that CO will be the main gaseous product of the hydrodecarbonization reaction.[39] Comparing the variation of CO and CO_2 concentrations, it was found that the decarboxylation effect of molybdenum disulfide is slightly higher (1−5 times) than the decarbonylation effect.[41]

Hydrodesulfurization can be considered the most efficient technique to remove sulfur from oil, resulting in clean hydrocarbons.[63−68] In this context, MoS_2 proved to be an effective catalytic material for the hydrodesulfurization reaction. Nickel nanoparticles deposited on the surface of molybdenum disulfide were used as an efficient catalytic material for the hydrodesulfurization of nickel and its derivatives.[69−71] Ni-MoS_2-based nanocomposites were synthesized by a solution chemistry method through a two-step approach. The particle size of the composites was determined based on MoS_2/Ni ratio, concentration, and temperature. 50.2 wt % of the catalytic system exhibited the highest catalytic performance with 99%, 98%, and 94% conversion of thiophene, benzothiophene, and dibenzothiophene, respectively.[72] Del Valle et al. concluded that exfoliated MoS_2 is more HDS active than crystalline MoS_2. The catalytic activity of crystalline MoS_2 exfoliated MoS_2, and MoS_2 was prepared from molybdenum naphthenate and ammonium heptamolybdate for the same HDS reactions. When crystallized and stripped MoS_2 was used, the yield of biphenyl was higher than that of tetrahydrodibenzomethine for all dibenzothiophene transformations. In addition, higher yields of trihydrodibenzothiophene were obtained when the other two catalysts were used. In the HDS of dibenzothiophene, MoS_2 derived from ammonium heptamolybdate exhibited higher catalytic activity than MoS_2 derived from molybdenum naphthenate.[73] Seyyedmajid et al. prepared the magnetic catalyst $MoS_2/SiO_2/Fe_3O_4$ by mixed micellar polymerization and hydrothermal synthesis, and the addition of surfactants CTAC and SDS during the preparation resulted in MoS_2 crystals of small size. Its high dispersion in the catalyst resulted in more than twice the desulfurization performance without the addition of surfactants,[40] and the direct desulfurization activity (DDS) of molybdenum disulfide was found to be much higher than the hydrodesulfurization (HDS) activity.[40] Quantum chemical techniques have shown that the chemisorption of hydrogen molecules on valence-unsaturated Mo atoms leads to H−H bond breakage and migration of H atoms to other valence-unsaturated Mo and S atoms. The study of the interaction of H_2S molecules with Mo_2S_4 and Mo_3S_6 clusters shows that the chemisorption of H_2S molecules occurs on valence-unsaturated Mo atoms, followed by the extraction and migration of H atoms on the cluster surface, with unsaturated S atoms playing the role of donors and hydrogen carriers. The results showed that sulfur-containing compounds (mercaptans, thiophenes, and dibenzothiophenes) are also chemisorbed via S atoms on valence-unsaturated Mo atoms located on the surface of MoS_2 clusters.[74] Hydrotreating of this complex feedstock was performed in an intermittent reactor using dispersed MoS_2 catalysts. The reactivity of different sulfides in light cycle oil followed the trend of benzothiophene > 1-methyl benzothiophene≫ 2-methyl benzothiophene > 3-methyl benzothiophene > 4-methyl benzothiophene ≫ dibenzothiophene ≈ 1-methyldibenzothiophenol ≈ 2-methyldibenzothiophenol ≈ 3-methyldibenzothiophenol. The removal of nitrogen compounds from LCO followed the trend of aniline > indole > carbazole.[38] Both theoretical calculations and experimental studies have shown that the ligand-unsaturated Mo sites on the surface of MoS_2 catalysts are active species in hydrodesulfurization catalysis. For example, density flooding theory studies suggest that the unsaturated molybdenum atoms exposed on the MoS_2 surface are responsible for the high activity of the HDS reaction.[75] Experimental results confirmed that the coordinated unsaturated Mo species are the active centers of molybdenum sulfide catalysts loaded on Al_2O_3 and TiO_2 for the hydrodesulfurization of thiophene and the hydrogenation of butadiene. Also, XPS results show that nano-MoS_2 shows a redshift of 0.2 eV compared to commercial MoS_2. This indicates that nano-MoS_2 has a higher amount of low Mo valence state, which implies a more coordinated unsaturated Mo site on the MoS_2 microfluidic surface.[43] Guo et al. synthesized MoCoS and MoNiS monolayers as catalysts for HDS and HDN in one step. The monolayer structure of MoS_2 ensures better activity for basic catalysts due to the high density of active centers. In HDS and HDN, the monolayer metal oxide semiconductor shows enhanced catalytic activity compared to the multilayer MoS. Rationally, cobalt-based MoS catalysts show higher conversions than nickel-based MoS in HDS, which is the counterpart of HDN.[44]

The unloaded MoCo(Ni)S catalysts also performed better in HDS and HDN compared to the conventional loaded catalysts.[76−78] Therefore, the one-step synthesis of carrier-free Mo(W)Co(Ni)S catalysts with well-defined structures has great potential to improve their catalytic performance in HDS and HDN reactions. Kun et al. studied the interaction effect between HDS and HDN under the catalysis of different Mo series catalysts,[44] proving the superiority of nitrogen-containing organic matter in hydrogenation.[79−81] In the presence of Ni, the adsorption effect of nitrogen-containing organic matter on the catalyst will be better.[82,83] The opening rate of Ni-MoS_2 under γ-Al_2O_3 loading is the best, while the opening rate of Ni/MoS_2 under unloading is the lowest. The HDN reaction was temperature dependent: as the temperature increased, due to the presence of Ni, the reaction with γ-Al_2O_3-loaded Ni-MoS_2 also showed a higher removal rate compared to Al_2O_3-loaded Ni-MoS_2.[84] For polymetallic catalysts, such as Ni−Mo−W, the simultaneous presence of Mo and W in the same slab hinders the growth of pro-Ni species and favors nucleation, which allows the largest fraction of Ni to be bound. In addition, the slow growth in the *Z*-direction leads to the maximization of active sites around the particles. Compared to bimetallic catalysts, trimetallic catalysts have the highest concentration of active centers and larger specific perimeters, leading to the highest rates of hydrodenitrogenation and hydrodesulfurization.[85]

The differences in catalytic properties are caused not only by the different properties of metals and auxiliary materials but also by the purity of the feedstock. For example, K in the feedstock causes an increase in the electronic charge on the MoS_2 material, raises the surface alkalinity, and blocks the Mo and S edges, inhibiting the catalytic activity and limiting the access of hydrogen to the MoS_2 surface. In particular, the decrease in HDS and HDO activity and the slight decrease in hydrogenation activity are related.[39]

6. CONCLUSION

Slurry bed reactors have recently gained momentum in the field of heavy oil hydrogenation because they overcome the challenges of pressure drop and mass transfer limitations present in conventional fixed-bed reactors and other reactors. As one of the important hydrogenation catalysts in slurry beds, the literature has focused on the reduction of the number of MoS_2 stacking layers, but there are a lack of studies on the lateral dimensions, microdomain regions, and defect sites. The relationship between molybdenum disulfide structure and hydrogenation effect also lags far behind the application of MoS_2 in hydrogen precipitation, etc. The current studies mostly focus on the variation of hydrogenation performance but lack detailed studies on active hydrogen transfer, etc. In slurry bed hydrogenation applications, oil-soluble molybdenum is a hot topic of research, but all need to be converted to a solid state to have hydrogenation activity. How does the conversion of soluble molybdenum-based catalysts to solid molybdenum disulfide during heavy oil hydrogenation positively affect the effect of heavy oil hydrogenation? This question is still unclear and poses a significant obstacle to reducing the cost of soluble Mo precursors and affecting their industrialization.

AUTHOR INFORMATION

Corresponding Author

Xueli Huang − *School of Chemical Engineering and Technology, Xinjiang University, Urumqi 830046, People's Republic of China*; Email: 1817280187@qq.com

Authors

Xiaoning Zhang − *School of Chemical Engineering and Technology, Xinjiang University, Urumqi 830046, People's Republic of China*; orcid.org/0009-0006-3895-1612

Buning Chen − *Xinjiang Xuanli Environmental Energy Co., Hami 839300, People's Republic of China*

Jianwei Wang − *Xinjiang Xuanli Environmental Energy Co., Hami 839300, People's Republic of China*

Yusheng Zhou − *Xinjiang Xuanli Environmental Energy Co., Hami 839300, People's Republic of China*

He Huang − *School of Chemical Engineering and Technology, Xinjiang University, Urumqi 830046, People's Republic of China*

Xuefeng Wang − *School of Chemical Engineering and Technology, Xinjiang University, Urumqi 830046, People's Republic of China*

Kaihong Li − *Sinopec Karamay Petrochemical Co. Ltd., Karamay 834000, People's Republic of China*

Complete contact information is available at:
https://pubs.acs.org/10.1021/acsomega.3c02029

Notes

The authors declare no competing financial interest.

ACKNOWLEDGMENTS

This work was financially supported by the Major Science and Technology Special Projects in the Autonomous Region (No. 2021A01002-2).

REFERENCES

(1) Sahu, R.; Song, B. J.; Im, J. S.; Jeon, Y.-P.; Lee, C. W. A review of recent advances in catalytic hydrocracking of heavy residues. *Journal of Industrial and Engineering Chemistry* **2015**, *27*, 12−24.

(2) Gang, Y.; Zhang, X.; Lei, X.; Guo, H.; Li, W.; Li, D. Hydroprocessing of low-temperature coal tar to produce jet fuel. *RSC Adv.* **2018**, *8*, 23663−23670.

(3) Huang, R.; Yuan, X.; Yan, L.; Han, L.; Bao, W.; Chang, L.; Liu, J.; Wang, J.; Ok, Y. S. Carbon precursors in coal tar: Extraction and preparation of carbon materials. *Sci. Total Environ.* **2021**, *788*, 147697.

(4) Pei, L.; Li, D.; Liu, X.; et al. Investigation on Asphaltenes Structures during Low-Temperature Coal Tar Hydrotreatment under Various Reaction Temperatures. *Energy Fuels* **2017**, *31*, 4705−4713.

(5) Wang, D.; Li, J.; Ma, H.; Yang, C.; Pan, Z.; Qu, W.; Tian, Z. Layer-structure adjustable MoS_2 catalysts for the slurry-phase hydrogenation of polycyclic aromatic hydrocarbons. *J. Energy Chem.* **2021**, *63*, 294−304.

(6) Yuan, Y.; Li, D.; Zhang, L.; Zhu, Y.; Wang, L.; Li, W. Development, Status, and Prospects of Coal Tar Hydrogenation Technology. *Energy Technology* **2016**, *4*, 1338−1348.

(7) Yang, T.-L.; Ni, S.-F.; Qin, P.; Dang, L. A mechanism study on the hydrogen evolution reaction catalyzed by molybdenum disulfide complexes. *Chem. Commun.* **2018**, *54*, 1113−1116.

(8) Du, H.-L.; Hodgetts, R. Y.; Chatti, M.; Nguyen, C. K.; Macfarlane, D. R.; Simonov, A. N.; et al. Is Molybdenum Disulfide Modified with Molybdenum Metal Catalytically Active for the Nitrogen Reduction Reaction. *J. Electrochem. Soc.* **2020**, *167*, 146507.

(9) Backes, C.; Higgins, T. M.; Kelly, A.; et al. Guidelines for exfoliation, characterization, and processing of layered materials produced by liquid exfoliation. *Chem. Mater.* **2017**, *29*, 243−255.

(10) Li, Y.; Zhang, Y.; Tong, X.; Wang, X.; Zhang, L.; Xia, X.; Tu, J.; et al. Recent progress on the phase modulation of molybdenum disulfide/diselenide and their applications in electrocatalysis. *Journal of Materials Chemistry A* **2021**, *9*, 1418−1428.

(11) Tan, J.; Zhang, W.; Shu, Y.; et al. Interlayer engineering of molybdenum disulfide toward efficient electrocatalytic hydrogenation. *Science Bulletin* **2021**, *66*, 1003−1012.

(12) Singh, A.; Moun, M.; Singh, R. Effect of different precursors on CVD growth of molybdenum disulfide. *J. Alloys Compd.* **2019**, *782*, 772−779.

(13) Huang, Y.; Yu, K.; Li, H.; et al. Scalable Fabrication of Molybdenum Disulfide Nanostructures and their Assembly. *Adv. Mater.* **2020**, *32*, 2003439.

(14) Kang, K. H.; Kim, G. T.; Park, S.; et al. A review on the Mo-precursors for catalytic hydroconversion of heavy oil. *Journal of Industrial and Engineering Chemistry* **2019**, *76*, 1−16.

(15) Lu, H.; Kummel, A.; Robertson, J. Passivating the sulfur vacancy in monolayer MoS_2. *APL Materials* **2018**, *6*, 066104.

(16) Gupta, D.; Chauhan, V.; Kumar, R. A comprehensive review on synthesis and applications of molybdenum disulfide (MoS) Material: Past and Recent Developments. *Inorg. Chem. Commun.* **2020**, *121*, 108200.

(17) Toh, R. J.; Sofer, Z.; Luxa, J.; et al. 3R phase of MoS_2 and WS_2 outperforms the corresponding 2H phase for hydrogen evolution. *Chem.Commun.* **2017**, *53*, 3054−3057.

(18) Samy, O.; El Moutaouakil, A. A Review on MoS_2 Energy Applications: Recent Developments and Challenges. *Energies* **2021**, *14*, 4586.

(19) Krishnan, U.; Kaur, M.; Singh, K.; et al. A synoptic review of MoS_2: Synthesis to applications. *Superlattices Microstruct.* **2019**, *128*, 274−297.

(20) Daage, M.; Chianelli, R. Structure-function relations in molybdenum sulfide catalysts: the″ rim-edge″ model. *J. Catal.* **1994**, *149*, 414−427.

(21) Lauritsen, J.; Helveg, S.; Lægsgaard, E.; et al. Atomic-scale structure of Co−Mo−S nanoclusters in hydrotreating catalysts. *J. Catal.* **2001**, *197*, 1−5.

(22) Schachtl, E.; Kondratieva, E.; Gutiérrez, O. Y.; et al. Pathways for H_2 activation on (Ni)-MoS_2 catalysts. *J. Phys. Chem. Lett.* **2015**, *6*, 2929−2932.

(23) Topsoe, N.; Topsoe, H. FTIR studies of Mo/Al_2O_3-based catalysts: II. Evidence for the presence of SH groups and their role in acidity and activity. *J. Catal.* **1993**, *139*, 641−651.

(24) Breysse, M.; Furimsky, E.; Kasztelan, S.; et al. Hydrogen activation by transition metal sulfides. *Catalysis Reviews* **2002**, *44*, 651−735.

(25) Travert, A.; Nakamura, H.; Vansanten, R. A.; et al. Hydrogen activation on Mo-based sulfide catalysts, a periodic DFT study. *J. Am. Chem. Soc.* **2002**, *124*, 7084−7095.

(26) Sun, M.; Nelson, A. E.; Adjaye, J. Ab initio DFT study of hydrogen dissociation on MoS_2, NiMoS, and CoMoS: mechanism, kinetics, and vibrational frequencies. *J. Catal.* **2005**, *233*, 411−421.

(27) Afanasiev, P.; Jobic, H. On hydrogen adsorption by nanodispersed MoS_2-based catalysts. *J. Catal.* **2021**, *403*, 111−120.

(28) Alvarez-Ramirez, F.; Ruiz-Morales, Y. Island versus archipelago architecture for asphaltenes: polycyclic aromatic hydrocarbon dimer theoretical studies. *Fuel* **2013**, *27*, 1791−1808.

(29) Afanasiev, P. Synthetic approaches to the molybdenum sulfide materials. *Comptes Rendus Chimie* **2008**, *11*, 159−182.

(30) Lauritsen, J.; Besenbacher, F. Atom-resolved scanning tunneling microscopy investigations of molecular adsorption on MoS_2 and CoMoS hydrodesulfurization catalysts. *J. Catal.* **2015**, *328*, 49−58.

(31) Tuxen, A. K.; Füchtbauer, H. G.; Temel, B.; et al. Atomic-scale insight into adsorption of sterically hindered dibenzothiophenes on MoS_2 and Co−Mo−S hydrotreating catalysts. *J. Catal.* **2012**, *295*, 146−154.

(32) Schachtl, E.; Zhong, L.; Kondratieva, E.; et al. Understanding Ni Promotion of MoS_2/γ-Al_2O_3 and its Implications for the Hydrogenation of Phenanthrene. *J. Catal.* **2015**, *7*, 4118−4130.

(33) Salazar, N.; Rangarajan, S.; Rodriguez-Fernandez, J.; Mavrikakis, M.; Lauritsen, J. V.; et al. Site-dependent reactivity of MoS_2 nanoparticles in hydrodesulfurization of thiophene. *Nat. Commun.* **2020**, *11*, 1−9.

(34) Zheng, P.; Xiao, C.; Cao, Z.; et al. DFT insights into the hydrodesulfurization mechanisms of different sulfur-containing compounds over CoMoS active phase: Effect of the brim and CUS sites. *Chem. Eng. Sci.* **2021**, *231*, 116311.

(35) Iwata, Y.; Araki, Y.; Honna, K.; et al. Hydrogenation active sites of unsupported molybdenum sulfide catalysts for hydroprocessing heavy oils. *Catal. Today* **2001**, *65*, 335−341.

(36) Yang, Z.; Zhu, L.; Lv, C.; et al. Defect engineering of molybdenum disulfide for energy storage. *Materials Chemistry Frontiers* **2021**, *5*, 5880−5896.

(37) Tajik, S.; Shahrabadi, A.; Rashidi, A. Silica-graphene nanohybrid supported MoS_2 nanocatalyst for hydrogenation reaction and upgrading heavy oil. *J. Pet. Sci. Eng.* **2019**, *177*, 822−828.

(38) Zhang, H.; Lin, H.; Zheng, Y. Hydrotreatment of Light Cycle Oil Over a Dispersed MoS_2 Catalyst. *International Journal of Chemical Reactor Engineering* **2016**, *14*, 703−711.

(39) Plaola, Y.; Leangsiri, W.; Pongsiriyakul, K.; Kiatkittipong, W.; Srifa, A.; Lim, J. W.; Reubroycharoen, P.; Kiatkittipong, K.; Eiad-ua, A.; Assabumrungrat, S.; et al. Catalytic Hydrotreating of Crude Pongamia pinnata Oil to Bio-Hydrogenated Diesel over Sulfided NiMo Catalyst. *Energies* **2022**, *15*, 1547.

(40) Sharifvaghefi, S.; Zheng, Y. Development of a Magnetically Recyclable Molybdenum Disulfide Catalyst for Direct Hydrodesulfurization. *ChemCatChem.* **2015**, *7*, 3397−3403.

(41) Zhang, Y.; Monnier, J.; Ikura, M. Bio-oil upgrading using dispersed unsupported MoS2 catalyst. *Fuel Process. Technol.* **2020**, *206*, 106403.

(42) Cuesta, J. D.; Leyva, C.; Lartundo, L.; et al. Hydrothermal synthesis of unsupported MoS_2 as catalyst for hydrodesulfurization of gas oil. *Petroleum Science and Technology* **2016**, *34*, 1720−1725.

(43) Li, Z.; Zhang, D.; Ma, J.; et al. Fabrication of MoS_2 microflowers for hydrogenation of nitrobenzene. *Mater. Lett.* **2018**, *213*, 350−353.

(44) Guo, K.; Ding, Y.; Yu, Z. One-step synthesis of ultrafine MoNiS and MoCoS monolayers as high-performance catalysts for hydrodesulfurization and hydrodenitrogenation. *Appl. Catal. B: Environmental* **2018**, *239*, 433−440.

(45) Mullins, O. C. Review of the Molecular Structure and Aggregation of Asphaltenes and Petroleomics. *SPE Journal* **2008**, *13* (01), 48−57.

(46) Mullins, O. C. The modified Yen model. *Energy&Fuels* **2010**, *24*, 2179−2207.

(47) Kadiev, K. M.; Gyul'maliev, A. M.; Kadieva, M. K.; Khadzhiev, S. N.; Batov, A. E.; et al. Quantum-Chemical and Experimental Investigation of the Catalytic Activity of Nanosized Particles of Nickel-Promoted Molybdenum Disulfide in the Hydroconversion Process. *Petroleum Chemistry* **2018**, *58*, 638−645.

(48) Schacht-Hernandez, P.; Portales-Martinez, B.; Laredo, G. C.; Perez-Romo, P.; Dominguez-Esquivel, J. M.; et al. Homogeneous catalyst for in-situ hydrotreating of heavy oils. *Appl. Catal. A: General* **2019**, *577*, 99−106.

(49) Choudhary, T. V.; Parrott, S.; Johnson, B. Unraveling heavy oil desulfurization chemistry: targeting clean fuels. *Environ. Sci. Technol.* **2008**, *42*, 1944−1947.

(50) Schachtl, E.; Yoo, J. S.; Gutiérrez, O. Y.; et al. Impact of Ni promotion on the hydrogenation pathways of phenanthrene on $MoS_2/\gamma\text{-}Al_2O_3$. *J. Catal.* **2017**, *352*, 171−181.

(51) Li, C.; Du, J.; Yang, T.; et al. Exploratory Investigation on the Slurry-Phase Hydrocracking Reaction Behavior of Coal Tar and Petroleum-Based Heavy Oil Mixed Raw Material. *Energy & Fuel* **2019**, *33*, 8471−8482.

(52) Li, C.; Han, Y.; Yang, T.; et al. Preliminary study on the influence of catalyst dosage on coke formation of heavy oil slurry-bed hydrocracking. *Fuel* **2020**, *270*, 117489.

(53) Liu, B.; Zhao, K.; Chai, Y.; et al. Slurry phase hydrocracking of vacuum residue in the presence of presulfided oil-soluble MoS_2 catalyst. *Fuel* **2019**, *246*, 133−140.

(54) Yusuf, A.; Al-Hajri, R. S.; Al-Waheibi, Y. M.; Jibril, B. Y.; et al. In-situ upgrading of Omani heavy oil with catalyst and hydrogen donor. *Journal of Analytical and Applied Pyrolysis* **2016**, *121*, 102−112.

(55) Prado, G. H. C.; Rao, Y.; de Klerk, A.; et al. Nitrogen removal from oil: a review. *Fuel* **2017**, *31*, 14−36.

(56) Guo, K.; Li, H.; Yu, Z. In-situ heavy and extra-heavy oil recovery: A review. *Fuel* **2016**, *185*, 886−902.

(57) Bui, V. N.; Laurenti, D.; Afanasiev, P.; et al. Hydrodeoxygenation of guaiacol with CoMo catalysts. Part I: Promoting effect of cobalt on HDO selectivity and activity. *Appl. Catal. B: Environmental* **2011**, *101*, 239−245.

(58) Whiffen, V.; Smith, K. Hydrodeoxygenation of 4-Methylphenol over Unsupported MoP, MoS2, and MoOx Catalysts. *Energy Fuels* **2010**, *24*, 4728−4737.

(59) Yoosuk, B.; Tumnantong, D.; Prasassarakich, P. Unsupported MoS_2 and $CoMoS_2$ catalysts for hydrodeoxygenation of phenol. *Chem. Eng. Sci.* **2012**, *79*, 1−7.

(60) Song, W.; Nie, T.; Lai, W.; et al. Tailoring the morphology of Co-doped MoS_2 for enhanced hydrodeoxygenation performance of p-cresol. *CrystEngComm* **2018**, *20*, 4069−4074.

(61) Wang, W.; Zhang, K.; Li, L.; et al. Synthesis of highly active Co−Mo−S unsupported catalysts by a one-step hydrothermal method for p-cresol hydrodeoxygenation. *E.C Research* **2014**, *53*, 19001−19009.

(62) Li, Q.; Bai, X.; Ling, C.; et al. Forming atom−vacancy interface on the MoS2 catalyst for efficient hydrodeoxygenation reactions. *Small Methods* **2019**, *3*, 1800315.

(63) Ali, I.; Saleh, T. A. Molybdenum boron based catalysts loaded on MnO alumina support for hydrodesulfurization of dibenzothiophene. *Inorg. Chem. Commun.* **2022**, *138*, 109237.

(64) Saleh, T. A. Carbon nanotube-incorporated alumina as a support for MoNi catalysts for the efficient hydrodesulfurization of thiophenes. *Chem. Eng. J.* **2021**, *404* (1), 126987.

(65) Ali, I.; Saleh, T. A. Zeolite-graphene composite as support for molybdenum-based catalysts and their hydrodesulfurization performance. *Appl. Catal. A: General* **2020**, *598*, 117542.

(66) Ali, I.; Al-Arfaj, A. A.; Saleh, T. A. Carbon nanofiber-doped zeolite as support for molybdenum based catalysts for enhanced hydrodesulfurization of dibenzothiophene. *J. Mol. Liq.* **2020**, *304*, 112376.

(67) Al-Jamimi, H. A.; Saleh, T. A. Transparent predictive modeling of catalytic hydrodesulfurization using an interval type-2 fuzzy logic. *Journal of Cleaner Production* **2019**, *231*, 1079−1088.

(68) Saleh, T. A. Simultaneous adsorptive desulfurization of diesel fuel over bimetallic nanoparticles loaded on activated carbon. *Journal of Cleaner Production* **2018**, *172*, 2123−2132.

(69) Danmaliki, G. I.; Saleh, T. A. Effects of bimetallic Ce/Fe nanoparticles on the desulfurization of thiophenes using activated carbon. *Chemical engineering journal* **2017**, *307*, 914−927.

(70) Saleh, T. A. Protocols for synthesis of nanomaterials, polymers, and green materials as adsorbents for water treatment technologies. *Environmental Technology & Innovation* **2021**, *24*, 101821.

(71) Saleh, T. A. Nanomaterials: Classification, properties, and environmental toxicities. *Environmental Technology & Innovation* **2020**, *20* (11), 101067.

(72) Cheng, F.; Chen, J.; Gou, X. MoS_2−Ni nanocomposites as catalysts for hydrodesulfurization of thiophene and thiophene derivatives. *Adv. Mater.* **2006**, *18*, 2561−2564.

(73) Tye, C. T.; Smith, K. J. Hydrodesulfurization of dibenzothiophene over exfoliated MoS_2 catalyst. *Catal. Today* **2006**, *116*, 461−468.

(74) Kadiev, K. M.; Gyul'maliev, A. M.; Kadieva, M. K. On the Mechanism of Sulfur Removal during Hydroconversion in the Presence of a Catalyst MoS_2. *Russian Journal of Applied Chemistry* **2021**, *94*, 518−527.

(75) Paul, J. F.; Payen, E. J. Vacancy formation on MoS_2 hydrodesulfurization catalyst: DFT study of the mechanism. *J. Phys. Chem. B* **2003**, *107*, 4057−4064.

(76) Ho, T. C.; McConnachie, J. M. Ultra-deep hydrodesulfurization on MoS_2 and Co0. $1MoS_2$: Intrinsic vs. environmental factors. *J. Catal.* **2011**, *277*, 117−122.

(77) Yi, Y.; Zhang, B.; Jin, X.; et al. Unsupported NiMoW sulfide catalysts for hydrodesulfurization of dibenzothiophene by thermal decomposition of thiosalts. *J. Mol. Catal. A: Chem.* **2011**, *351*, 120−127.

(78) Yoosuk, B.; Song, C.; Kim, J. H.; et al. Effects of preparation conditions in hydrothermal synthesis of highly active unsupported NiMo sulfide catalysts for simultaneous hydrodesulfurization of dibenzothiophene and 4, 6-dimethyldibenzothiophene. *Catal. Today* **2010**, *149*, 52−61.

(79) Egorova, M.; Prins, R. The role of Ni and Co promoters in the simultaneous HDS of dibenzothiophene and HDN of amines over Mo/γ-Al_2O_3 catalysts. *J. Catal.* **2006**, *241*, 162−172.

(80) Ho, T. C.; Qiao, L. Competitive adsorption of nitrogen species in HDS: Kinetic characterization of hydrogenation and hydrogenolysis sites. *J. Catal.* **2010**, *269*, 291−301.

(81) Zepeda, T.; Pawelec, B.; Estrella, R.; et al. Competitive HDS and HDN reactions over NiMoS/HMS-Al catalysts: Diminishing of the inhibition of HDS reaction by support modification with P. *Appl. Catal. B: Environmental* **2016**, *180*, 569−579.

(82) Rangarajan, S.; Mavrikakis, M. On the preferred active sites of promoted MoS_2 for hydrodesulfurization with minimal organonitrogen inhibition. *ACS Catal.* **2017**, *7*, 501−509.

(83) Rangarajan, S.; Mavrikakis, M. DFT insights into the competitive adsorption of sulfur-and nitrogen-containing compounds and hydrocarbons on Co-promoted molybdenum sulfide catalysts. *ACS Catal.* **2016**, *6*, 2904−2917.

(84) Hein, J.; Hrabar, A.; Jentys, A.; et al. γ-Al_2O_3-Supported and Unsupported (Ni)MoS_2 for the Hydrodenitrogenation of Quinoline in the Presence of Dibenzothiophene. *ChemCatChem.* **2014**, *6*, 485−499.

(85) Hein, J.; Gutiérrez, O. Y.; Schachtl, E.; et al. Distribution of Metal Cations in Ni-Mo-W Sulfide Catalysts. *ChemCatChem.* **2015**, *7*, 3692−3704.